Inorganic Chemistry

Communication

pubs.acs.org/IC

Dumbbells of Five-Connected Ge Atoms and Superconductivity in $CaGe_3$

Walter Schnelle, Alim Ormeci, Aron Wosylus,[†] Katrin Meier, Yuri Grin, and Ulrich Schwarz*

Max-Planck-Institut für Chemische Physik fester Stoffe, Dresden, Germany

Supporting Information

ABSTRACT: $CaGe_3$ has been synthesized at high-pressure, high-temperature conditions. The atomic pattern comprises intricate germanium layers of condensed moleculelike dimers. Below T_c = 6.8 K, type II superconductivity with moderately strong electron−phonon coupling is observed.

Covalent bonding in strongly polar intermetallic compounds plays a key role in the understanding of the interplay between spatial organization of solids and their electronic structure. Discrete species like clusters, dumbbells, chains, columns, layers, or frameworks have triggered the development of basic electron-counting schemes like the Wade rules[1] or the Zintl concept.[2] However, interestingly, compounds violating the conditions for electron-precise frameworks fulfill the requirements for covalent metals with fascinating and potentially useful properties like superconductivity or thermoelectricity.[3] For example, the germanide Ba_6Ge_{25} (T_c = 0.24 K[4]) comprises a framework of three- and four-bonded Ge atoms. According to the 8 − N rule, this connectivity of the germanium partial structure corresponds to $(3b)Ge^-$ and uncharged species $(4b)Ge^0$. With the oxidation state 2+ for barium, this yields an excess of four electrons per formula unit, $(Ba^{2+})_6[(3b)Ge^-]_8[(4b)Ge^0]_{17}\cdot 4e^-$.

A different strategy to obtain a sufficient carrier concentration is the realization of unusual coordination environments in the covalent partial structure by the application of high pressure.[5,6] Examples for germanium connectivities exceeding the scope of the 8 − N rule are pentagermanides $LnGe_5$ (Ln = La, Ce, Pr, Nd, Sm, Gd, Tb[7]) with coordination number (CN) 5 and 8 or the recently synthesized $BaGe_3$[8] with CN 6. Herein, we report on the high-pressure synthesis of $CaGe_3$ by annealing mixtures of $CaGe_2$ and Ge($cF8$) at 10(1) GPa and 1200(120) K for 1 h before quenching.[9] The reaction product $CaGe_3$ is metastable at ambient pressure and contains only traces of an unidentified phase. $CaGe_3$ is the first germanide adopting this atomic arrangement.

The atomic pattern of $CaGe_3$[10] consists of two-dimensional germanium units that are separated by Ca atoms (Figure 1). The complex germanium layers comprise two different crystallographic positions. Dimer units $(Ge2)_2$ are arranged parallel to the c axis in the form of square prisms that are braced by $(Ge1)_2$ pairs in two perpendicular orientations. This linking results in (001)-oriented infinite slabs of condensed dumbbells. Both germanium species, Ge1 and Ge2, adopt 1 + 4 homonuclear contacts.

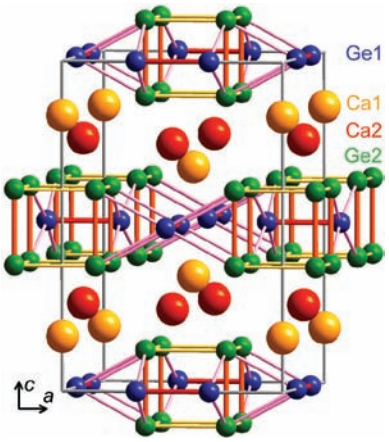

Figure 1. Projection of the crystal structure of $CaGe_3$. Within the germanium layers, short distances of 254.9(1) pm and of 259.94(8) pm are displayed as red and orange lines, respectively. Longer contacts of 276.31(5) and 282.31(7) pm are shown as pink and yellow, respectively. The crystallographic unit cell is indicated by gray lines.

The atomic coordination makes a contribution to the interatomic distances owing to the Pauli repulsion.[11] In order to single out the effect of the connectivity in germanium-rich compounds, average distances for various numbers of Ge−Ge contacts are investigated (Figure 2). The dashed curve corresponds to an empirical scaling for the heteronuclear near-neighbor distances in binary compounds.[11] The approach describes the experimentally observed average network distances for alkaline-earth and rare-earth metal germanides remarkably well. This is taken as an indication of the distinguished relevance of the homonuclear germanium interactions in these network structures. However, the significantly shorter distances for four-bonded Ge atoms in clathrate patterns reveal that the validity of the scaling is limited to frameworks with similar bonding properties and related metal−network interactions.

The connectivity of five for the Ge atoms clearly violates the 8 − N rule, demanding a more elaborate analysis of the chemical bonding. Computations of the electron localizability indicator (ELI)[12] within the local density approximation[13,14] reveal the formation of two-center bonds Ge1−Ge1 and Ge2−Ge2 in accordance with the shortest interatomic distances (see local maxima, indicated in white, between the Ge atoms in Figure 3, left and right). The attractors at the exterior of the

Received: March 19, 2012
Published: May 7, 2012

dx.doi.org/10.1021/ic300576a | *Inorg. Chem.* 2012, 51, 5509−5511

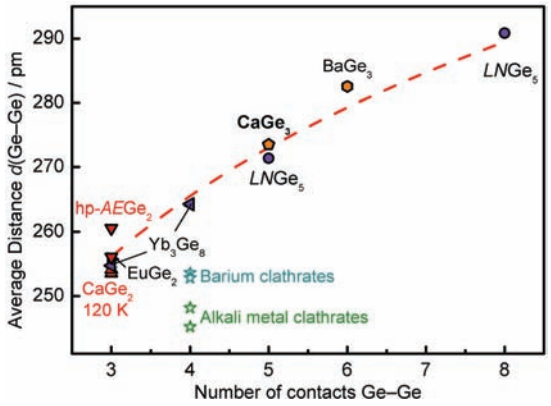

Figure 2. Interdependence of interatomic distances d(Ge−Ge) and the number of Ge−Ge contacts CN_H.[15] The selection considers compounds in which the pure germanium substructure is completely organized in the form of networks[7,16] and is complemented by recent data for $BaGe_3$[8] with columnar units. The dashed curve visualizes the scaling[11] $d = d_R(CN_H/CN_R)^{1/8}$. The reference distance d_R = 256.1 pm corresponds to the average value for germanium environments in compounds $AEGe_2$ (AE = Ca, Sr, Ba) with CN_R = 3.

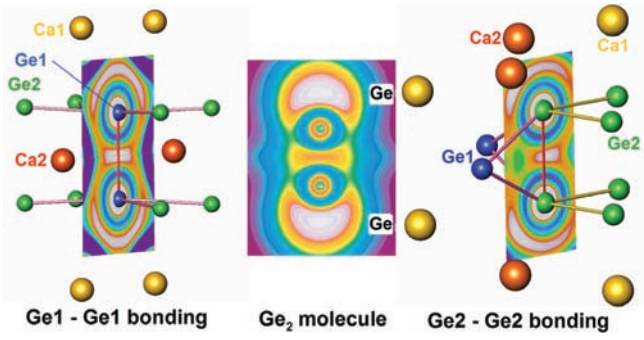

Figure 3. Bonding features of the five-connected Ge atoms in $CaGe_3$ visualized by the ELI-D distribution around the Ge_2 pairs (left and right) in comparison to the distribution of the electron localization function in the hypothetical molecule Ge_2 [middle; d(Ge−Ge) = 246 pm; orbital configuration $\sigma_g^2\sigma_u^2\pi_u^4\sigma_g^2$].[18]

dumbbell stand for lone-pair behavior in the isolated molecule Ge_2, and their respective basins have axial symmetry (Figure 3, middle). In $CaGe_3$, the shapes of the basins for these attractors deviate strongly from this situation. This reveals the influence of the neighboring Ca atoms on the Ge_2 units and represents multicenter Ca−Ge interactions. The fourth shell of the Ca atoms is to a large extent featureless in the ELI-D distribution, lending support to substantial charge transfer from Ca to the Ge_2 dumbbells. The five connectivity of the Ge atoms is supported by packing effects and undirected interactions rather than being caused by pure covalent bonding between the Ge_2 species. This finding is well in agreement with the bonding and connectivity in the modification Ge($hR8$).[17]

The room temperature resistivity of the present sample,[19] $\rho_{300\,K} \approx 136\ \mu\Omega$ cm, with its residual resistivity of $\rho_{0\,K} \approx 86\ \mu\Omega$ cm, is rather high, implying poor contact between the grains. A drop in the electrical resistivity indicates a transition into the superconducting state below 6.2 K. The magnetic susceptibility of a zero-field-cooled sample exhibits a strong diamagnetic signal (inset of Figure 4). For μ_0H = 2 mT, the transition temperature is determined by a tangent to the steepest slope of $\chi_{zfc}(T)$ resulting in T_c = 6.8(1) K. The shielded sample volume

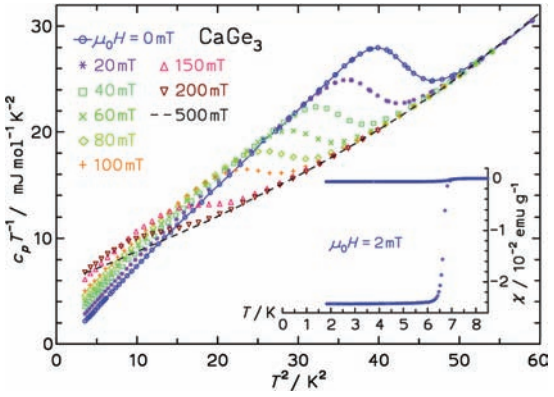

Figure 4. Specific heat capacity of $CaGe_3$ for different magnetic fields H plotted as c_p/T against T^2 (colored symbols). The data for μ_0H = 500 mT represent the normal conducting state (dashed line). The inset shows the magnetic susceptibility for a nominal field μ_0H = 2 mT showing the shielding and the Meissner effect.

suggests bulk superconductivity. The very small field-cooling Meissner effect (inset of Figure 4) is assigned to strong flux-line pinning in a hard type II superconductor.

At low temperatures, the specific heat $c_p(T)$ (Figure 4) shows a clear second-order-type phase transition that is affected by magnetic fields of less than 0.1 T. The appearance of this significant anomaly confirms the bulk character of the superconductivity in $CaGe_3$. The normal-state specific-heat data between 4.0 and 8.0 K measured in an overcritical field of 0.5 T are well fitted by the approach $c_N(T) = \gamma_N T + \beta T^3 + \delta T^5$. Here, γ_N is the electronic specific heat (Sommerfeld) coefficient and $\beta T^3 + \delta T^5$ are the first terms of the harmonic lattice approximation for the phonon contribution. The fit results in γ_N = 6.31(7) mJ mol^{-1} K^{-2}, and the value of β corresponds to an initial Debye temperature of $\Theta_D(0)$ = 330 K. The weak-coupling BCS theory falls far short to describe the difference specific heat $\Delta c = c_S(T) - c_{N,fit}(T)$ close to the critical temperature T_c. A fit using the phenomenological α model,[20] which scales the superconducting energy gap ΔE at the Fermi level E_F with the parameter $\alpha = \Delta E/k_BT_c$, describes the data quite well for α = 1.94(4) and γ = 5.6(2) mJ mol^{-1} K^{-2}. The value of α is significantly larger than that for the weak-coupling limit of the BCS theory (α = 1.76) and indicates that $CaGe_3$ is a superconductor with moderately strong electron−phonon coupling. Using the field dependence of the superconducting transition in $c_p(T)$, the upper critical field is estimated by a WHH extrapolation[21] to amount to $\mu_0H_{c2} \approx 290$ mT.

The computed density of states at E_F adds up to 1.49 states eV^{-1} per formula unit, which converts to a "bare" electronic specific heat coefficient γ_b = 3.5 mJ mol^{-1} K^{-2}. In conjunction with the experimental value γ_N, an electron−phonon coupling λ = 0.80 can be estimated by the relation $\gamma_N = (1 + \lambda)\gamma_b$ for the electron−phonon enhancement. Using the McMillan formula $\ln(1.45\ T_c/\Theta_D) = -1.04(1 + \lambda)/[\lambda - \mu^*(1 + 0.62\lambda)]$ with the common value of μ^* = 0.15, λ can also be evaluated from the ratio of the superconducting T_c and the Debye temperature Θ_D. With our experimental values, we obtain λ = 0.72, which is fairly close to the λ value estimated above. This agreement gives strong evidence that the superconductivity in $CaGe_3$ is phonon-mediated.

dx.doi.org/10.1021/ic300576a | Inorg. Chem. 2012, 51, 5509−5511

■ ASSOCIATED CONTENT

Supporting Information

Powder X-ray diffraction patterns, Rietveld refinement, displacement parameters, interatomic distance, microstructure of a $Ca_{25}Ge_{75}$ alloy, differential thermal analysis data, total and partial densities, and calculated isosurfaces. This material is available free of charge via the Internet at http://pubs.acs.org.

■ AUTHOR INFORMATION

Corresponding Author

*E-mail: schwarz@cpfs.mpg.de.

Present Address

†BASF AG, 67056 Ludwigshafen, Germany.

Notes

The authors declare no competing financial interest.

■ ACKNOWLEDGMENTS

We thank Susann Leipe for syntheses, Yurii Prots, Andreas Czulucki, and Irene Margiolaki (ESRF) for synchrotron X-ray diffraction experiments, Stefan Hoffmann and Susann Scharsach for differential thermal analysis measurements, and Ulrich Burkhardt for metallographic characterization.

■ REFERENCES

(1) Wade, K. *Adv. Inorg. Radiochem.* **1976**, *18*, 1.

(2) (a) Zintl, E.; Brauer, G. *Z. Phys. Chem.* **1933**, *B 20*, 245. (b) Zintl, E. *Angew. Chem.* **1939**, *52*, 1. (c) Schäfer, H.; Eisenmann, B.; Müller, W. *Angew. Chem., Int. Ed.* **1973**, *12*, 694.

(3) (a) Nolas, G. S.; Slack, G. A.; Schujman, S. B. In *Semiconductors and Semimetals*; Tritt, T. M., Ed.; Academic Press: San Diego, CA, 2000; Vol. *69*; p 255. (b) Kleinke, H. *Chem. Mater.* **2010**, *22*, 604.

(4) (a) Fukuoka, H.; Ueno, K.; Yamanaka, S. *J. Organomet. Chem.* **2000**, *611*, 543. (b) Grosche, F. M.; Yuan, H. Q.; Carillo-Cabrera, W.; Paschen, S.; Langhammer, C.; Kromer, F.; Sparn, G.; Baenitz, M.; Grin, Y.; Steglich, F. *Phys. Rev. Lett.* **2001**, *87*, 247003. (c) Yuan, H. Q.; Grosche, F. M.; Carillo-Cabrera, W.; Pacheco, V.; Sparn, G.; Baenitz, M.; Schwarz, U.; Grin, Y.; Steglich, F. *Phys. Rev.* **2004**, *B70*, 174512.

(5) Affronte, M.; Sanfilippo, S.; Nunez-Regueiro, M.; Laborde, O.; LeFloch, S.; Bordet, P.; Hanfland, M.; Levi, D.; Palenzona, A.; Olcese, G. L. *Physica B* **2000**, *284−288*, 1117.

(6) Evers, J.; Oehlinger, G.; Ott, H. R. *J. Less Common Met.* **1980**, *69*, 389.

(7) (a) Fukuoka, H.; Yamanaka, S. *Phys. Rev.* **2003**, *B67*, 094501. (b) Fukuoka, H.; Baba, K.; Yoshikawa, M.; Ohtsu, F.; Yamanaka, S. *J. Solid State Chem.* **2009**, *182*, 2024. (c) Meier, K.; Cardoso-Gil, R.; Schnelle, W.; Rosner, H.; Burkhardt, U.; Schwarz, U. *Z. Anorg. Allg. Chem.* **2010**, *636*, 1466.

(8) Fukuoka, H.; Tomomitsu, Y.; Inumaru, K. *Inorg. Chem.* **2011**, *50*, 6372.

(9) $CaGe_2$ is prepared by reacting Ca (Alpha Aesar, 99.987%) and Ge(*cF*8) (Alpha Aesar, 99.9999%) in an arc furnace. High pressures are generated by transforming directed forces of the hydraulic press into quasihydostatic conditions by a Walker module using MgO octahedra with 14 mm edge length. Heating under load is realized by resistive warming of the graphite sleeves girdling the boron nitride crucibles housing the samples. Pressure and temperature calibration has been performed prior to the experiments.

(10) Least-squares refinements of the structure model used full diffraction profiles with a pseudo-Voigt function in the Thompson−Cox−Hastings parametrization for the profile shape.[22] Computations included 356 reflections for 41 parameters and converged to R_p = 0.031, R_{wp} = 0.042, and R_{exp} = 0.019. $CaGe_3$ crystallizes in the tetragonal space group *I*4/*mmm* (No. 139) with a = 769.20(4) pm, c = 1133.14(9) pm, Z = 8: Ca1 [0, 0, 0.1655(2)], U_{iso} = 55(7) pm^2; Ca2 ($^1/_2$, 0, $^1/_4$), U_{iso} = 90(8) pm^2; Ge1 [0.3343(1), 0, 0], U_{iso} = 66(3) pm^2; Ge2 [0.31649(6), x, 0.11470(5)], U_{iso} = 128(2) pm^2. Further details of data collection, refinement, and interatomic distances are given in Tables S1−S3 and Figure S1 in the Supporting Information.

(11) Pauling, L. *The nature of the chemical bond and the structure of molecules and crystals*; Cornell University Press: Ithaca, NY, 1995.

(12) (a) Kohout, M. *Int. J. Quantum Chem.* **2004**, *97*, 651. (b) Kohout, M.; Wagner, F. R.; Grin, Yu. *Int. J. Quantum Chem.* **2006**, *106*, 1499. (c) Kohout, M. *Faraday Discuss.* **2007**, *135*, 43.

(13) (a) Jepsen, O.; Burkhardt, A.; Andersen, O. K. *The Program TB-LMTO-ASA*, version 4.7; Max-Planck-Institut für Festkörperforschung: Stuttgart, Germany, 1999. (b) Andersen, O. K. *Phys. Rev. B* **1975**, *12*, 3060. (c) von Barth, U.; Hedin, L. *J. Phys. (Paris)* **1972**, *C5*, 3060.

(14) (a) Koepernik, K.; Eschrig, H. *Phys. Rev.* **1999**, *B59*, 1743. (b) Perdew, J. P.; Wang, Y. *Phys. Rev.* **1992**, *B45*, 13244.

(15) Considered are interatomic distances in pure germanium networks of binary compounds MGe_x (M = main-group or lanthanide metal; $x \geq 2$) in which interatomic distances at ambient conditions have been determined by complete structure refinements. Atomic patterns exhibiting disorder or defects have not been considered; e.g., $ThSi_2$-, AlB_2-, and $GdSi_{1.4}$-type structures have been omitted because recent work evidences the presence of vacancies in the germanium sublattice and the formation of superstructures that are associated with a substantial reduction of the connectivity and changes of the interatomic distances. (a) Guloy, A. M.; Corbett, J. D. *Inorg. Chem.* **1991**, *30*, 4789. (b) Venturini, G.; Ijjaali, I.; Malaman, B. *J. Alloys Compd.* **1999**, *284*, 262. (c) Venturini, G.; Ijjaali, I.; Malaman, B. *J. Alloys Compd.* **1999**, *285*, 194. (d) Venturini, G.; Ijjaali, I.; Malaman, B. *J. Alloys Compd.* **1999**, *289*, 168.

(16) (a) Evers, J.; Oehlinger, G.; Weiss, A. *Z. Naturforsch.* **1980**, *B35*, 397. (b) Evers, J.; Oehlinger, G.; Weiss, A. *Z. Naturforsch.* **1977**, *B32*, 1352. (c) Tobash, P. H.; Bobev, S. *J. Solid State Chem.* **2007**, *180*, 1575. (d) Carrillo-Cabrera, W.; Curda, J.; von Schnering, H. G.; Paschen, S.; Grin, Yu. *Z. Kristallogr.-New Cryst. Struct.* **2000**, *215*, 207. (e) Kim, J.-H.; Okamoto, N. L.; Kishida, K.; Tanaka, K.; Inui, H. *J. Appl. Phys.* **2007**, *102*, 094506. (f) Fukuoka, H.; Iwai, K.; Yamanaka, S.; Abe, H.; Yoza, K.; Häming, L. *J. Solid State Chem.* **2000**, *151*, 117. (g) Gladyshevskii, E. I. *Dopov. Akad. Nauk Ukr. RSR* **1964**, 209. (h) Bobev, S.; Bauer, E. D.; Thompson, J. D.; Sarrao, J. L.; Miller, G. J.; Eck, B.; Dronskowski, R. *J. Solid State Chem.* **2004**, *177*, 3545. (i) Pani, M.; Palenzona, A. *J. Alloys Compd.* **2003**, *360*, 151. (j) Gallmeier, J.; Schäfer, H.; Weiss, A. *Z. Naturforsch.* **1969**, *B24*, 665. (k) Meier, K.; Koz, C.; Kerkau, A.; Schwarz, U. *Z. Kristallogr. NCS* **2009**, *224*, 349. (l) Meier, K.; Kerkau, A.; Schwarz, U. *Z. Kristallogr.-New Cryst. Struct.* **2009**, *224*, 373. (m) Carrillo-Cabrera, W.; Budnyk, S.; Prots, Yu.; Grin, Yu. *Z. Anorg. Allg. Chem.* **2004**, *630*, 2267. (n) Guloy, A. M.; Tang, Z.; Ramlau, R.; Böhme, B.; Baitinger, M.; Grin, Yu. *Eur. J. Inorg. Chem.* **2009**, 2455. (o) Evers, J.; Oehlinger, G.; Weiss, A. *Z. Naturforsch.* **1979**, *B34*, 524.

(17) Schwarz, U.; Wosylus, A.; Böhme, B.; Baitinger, M.; Hanfland, M.; Grin, Yu. *Angew. Chem., Int. Ed.* **2008**, *47*, 6790.

(18) Kohout, M.; Wagner, F. R.; Grin, Yu. *Theor. Chem. Acc.* **2002**, *108*, 150.

(19) The sample used for establishing the physical properties of $CaGe_3$ was a polycrystalline pellet (m = 66 mg). Magnetization was measured for fields $\mu_0 H$ between 2 mT and 7 T (1.8−300 K) in a SQUID magnetometer (MPMS XL-7, Quantum Design). Electrical resistance was determined by a direct-current four-probe method (4−320 K). Owing to the contact geometry, the inaccuracy of the electrical resistivity is estimated to be ±20%. The heat capacity was measured by a relaxation-type method (PPMS, Quantum Design) between 1.9 and 11 K in fields $\mu_0 H$ up to 0.5 T.

(20) Padamsee, H.; Neighbor, J. E.; Shiffman, C. A. *J. Low-Temperature Phys.* **1973**, *12*, 387.

(21) Werthammer, N. R.; Helfand, E.; Hohenberg, P. C. *Phys. Rev.* **1966**, *147*, 295.

(22) (a) Rodriguez-Carvajal, J. *Physica B* **1993**, *192*, 55. (b) Thompson, P.; Cox, D. E.; Hastings, J. B. *J. Appl. Crystallogr.* **1987**, *20*, 79. (c) Finger, L. W. *J. Appl. Crystallogr.* **1998**, *31*, 111.